Orientation of Intermediate Nucleotide States of Indane Dione Spin-Labeled Myosin Heads in Muscle Fibers

Osha Roopnarine and David D. Thomas
Department of Biochemistry, University of Minnesota Medical School, Minneapolis, Minnesota 55455 USA

ABSTRACT We have used electron paramagnetic resonance to study the orientation of myosin heads in the presence of nucleotides and nucleotide analogs, to induce equilibrium states that mimic intermediates in the actomyosin ATPase cycle. We obtained electron paramagnetic resonance spectra of an indane dione spin label (InVSL) bound to Cys 707 (SH1) of the myosin head, in skinned rabbit psoas muscle fibers. This probe is rigidly immobilized on the catalytic domain of the head, and the principal axis of the probe is aligned nearly parallel to the fiber axis in rigor (no nucleotide), making it directly sensitive to axial rotation of the head. On ADP addition, all of the heads remained strongly bound to actin, but the spectral hyperfine splitting increased by 0.55 ± 0.02 G, corresponding to a small but significant axial rotation of 7°. Adenosine 5′-(adenylylimidodiphosphate) (AMPPNP) or pyrophosphate reduced the actomyosin affinity and introduced a highly disordered population of heads similar to that observed in relaxation. For the remaining oriented population, pyrophosphate induced no significant change relative to rigor, but AMPPNP induced a slight but probably significant rotation (2.2° ± 1.6°), in the direction opposite that induced by ADP. Adenosine 5′-*O*-(3-thiotriphosphate) (ATPγS) relaxed the muscle fiber, completely dissociated the heads from actin, and produced disorder similar to that in relaxation by ATP. ATPγS plus Ca induced a weak-binding state with most of the actin-bound heads disordered. Vanadate had negligible effect in the presence of ADP, but in isometric contraction vanadate substantially reduced both force and the fraction of oriented heads. These results are consistent with a model in which myosin heads are disordered early in the power stroke (weak-binding states) and rigidly oriented later in the power stroke (strong-binding states), whereas transitions among the strong-binding states induce only slight changes in the axial orientation of the catalytic domain.

INTRODUCTION

A central hypothesis in muscle contraction is that force is generated by the reorientation of the myosin head (M) on actin (A) while coupled to the biochemical steps of the ATPase cycle (Scheme 1) (Huxley, 1969; Huxley and Simmons, 1971). It has been proposed that each kinetic state of nucleotide-bound myosin is characterized by a distinct axial orientational configuration (Morales and Botts, 1979). In rigor (no nucleotide), electron microscopy (EM) has shown clearly that myosin heads are highly oriented, approximately at a distinct 45° angle to the fiber axis (Reedy et al., 1965), and electron paramagnetic resonance (EPR) has shown that virtually all heads in the muscle fiber lie within a 15° range of axial (tilt) angles (Thomas and Cooke, 1980; Fajer et al., 1990b; Roopnarine and Thomas, 1994b). Despite significant efforts with structural and spectroscopic techniques, there is no compelling evidence for reorientation of myosin heads between two (or several) distinct angles during steady-state contraction. EPR has revealed that most of the myosin heads in contraction have a high degree of dynamic (microsecond) orientational disorder, with a small fraction of the heads in an orientation indistinguishable from rigor (Cooke et al., 1982; Thomas, 1987; Cooke, 1986; Fajer et al., 1991; Roopnarine and Thomas, 1995). This suggests that either the simple two-orientation model for contraction has to be replaced by one that includes more dynamic disorder, e.g., a disorder-to-order transition (Thomas et al., 1995), or the kinetic state that favors a distinct nonrigor orientation is not highly populated during steady-state contraction. The orientation of short-lived intermediate nucleotide states could be studied by detecting EPR signals during the transient phase of the ATPase cycle (Fajer et al., 1990c; Ostap et al., 1993; Roopnarine and Thomas, 1994a) or by using nucleotides and nucleotide analogs (Scheme 1, in boxes) to stabilize equilibrium states that may represent intermediates in the ATPase reaction sequence. In the present study, we focus on the latter approach, using nucleotide (ADP) and nucleotide analogs (AMPPNP, pyrophosphate, ATPγS, and ADP.vanadate) to study the orientation of nucleotide-bound myosin heads in both the weak and strong-binding actin states.

The AM·ADP state is formed by the addition of ADP in rigor (Sleep and Hutton, 1980; Dantzig and Goldman, 1985) and probably mimics a post-power-stroke state that follows the rate-limiting step of the ATPase kinetic cycle. EM studies show that the axial orientation of this state is indistinguishable from that of rigor (Reedy et al., 1965), and most spectroscopic probe studies also show only a slight orientational difference (Fajer et al., 1990b). The binding of AMPPNP (a nonhydrolyzable ATP analog) weakens the actin-myosin bond, but the resulting cross-bridge state is

Received for publication 21 July 1995 and in final form 28 February 1996.
Address reprint requests to Dr. David D. Thomas, Department of Biochemistry, University of Minnesota Medical School, Milard 4-225, 434 Delaware Street SE, Minneapolis, MN 55455. Tel.: 612-625-0957; Fax: 612-624-0632; E-mail: ddt@ddt.biochem.umn.edu.

Dr. Roopnarine's present address is Department of Molecular, Cellular, and Developmental Biology, University of Colorado, Boulder, CO 80309. E-mail: roopnari@stripe.colorado.edu.

0006-3495/96/06/2795/12 $2.00

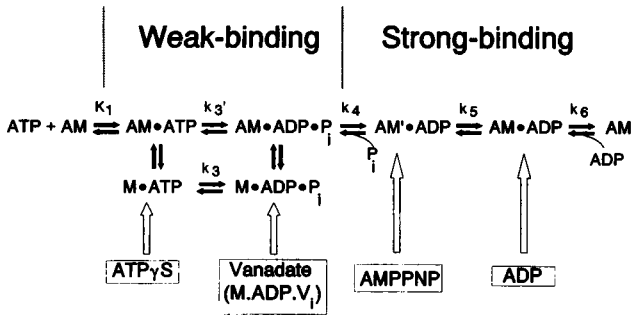

Scheme 1.

still termed "strongly bound" (Greene and Eisenberg, 1978) and may correspond to the force-generating intermediate state, AM'·ADP (Scheme 1). This state of intermediate actin-myosin affinity also has mechanical (Marston et al., 1976; Kuhn, 1978), structural (Barrington-Leigh et al., 1972; Goody et al., 1975; Reedy et al., 1983), and orientational (Fajer et al., 1988) properties intermediate between rigor and relaxation. Pyrophosphate is another nonhydrolyzable analog that mimics an intermediate state similar to that of AMPPNP (Cooke and Pate, 1988). It was recently shown that the phosphates in pyrophosphate occupy the same region in the ATP-binding site as an ATP analog (ADP·BeF) (Smith and Rayment, 1995). ATPγS is an ATP analog that mimics the weak-binding M·ATP state and is slowly hydrolyzed by myosin (Bagshaw et al., 1972). Mechanical, x-ray diffraction, and spectroscopic studies have shown that the M·ATPγS state has properties expected for weak-binding states in the ATPase cycle (Dantzig et al., 1988; Kraft et al., 1992; Xu et al., 1993; Berger and Thomas, 1994). Phosphate binding to the force-generating AM'ADP cross-bridge state reverses the cycle to produce a non-force-producing state (Dantzig et al., 1992). Vanadate is a phosphate analog, which in the presence of ADP traps myosin heads in a weak-binding state analogous to M·ADP·P_i (Scheme 1) (Goodno, 1979; Goodno and Taylor, 1982), although in muscle fibers this intermediate can be trapped only in the presence of ATP (Dantzig and Goldman, 1985; Ostap et al., 1995).

EPR spectroscopy is a uniquely powerful technique for studying the rotational dynamics and orientation of spin-labeled myosin heads (Thomas, 1987). Most of the EPR studies cited above have been done with an SH1 (Cys 707)-bound maleimide spin label (MSL: *N*-(1-oxy-2,2,6,6-tetramethyl-4-piperidinyl) maleimide), which has revealed no head orientation substantially different from rigor, except for weakly bound states that are dynamically disordered when bound to actin (reviewed by Thomas et al., 1995). We recently began studying the myosin head orientation with an indane-dione spin label, designated InVSL (Roopnarine et al., 1993, 1995; Roopnarine and Thomas, 1994a,b, 1995). EPR reports directly the orientation of the probe, not the protein, so it is difficult to distinguish a change in protein orientation from a probe rotation relative to the protein. However, InVSL has been shown to be rigidly immobilized on the myosin head, in both the presence and absence of nucleotides (Roopnarine et al., 1993), which makes it an ideal reporter of global myosin head rotations. InVSL is the only spin label that has been shown to bind to the myosin head with its principal axis aligned almost perfectly parallel to the muscle fiber axis, giving it a unique orientational perspective, and making it ideal for minimizing ambiguity in detecting axial head rotation (Roopnarine and Thomas, 1994b). In isometric contraction most of the heads are disordered, essentially as in relaxation, but 21% of the myosin heads are ordered essentially as in rigor (Roopnarine and Thomas, 1995), consistent with previous results obtained with MSL (Cooke et al., 1982). In the present study, we have used EPR spectroscopy of InVSL-labeled myosin heads in skinned rabbit psoas fibers to study the orientation of different intermediate states of myosin heads, induced by ADP, AMPPNP, pyrophosphate, ATPγS, and vanadate.

MATERIALS AND METHODS

Reagents and solutions

The spin label InVSL (Fig. 1 *A*) was synthesized by Hankovszky et al. (1989). Creatine kinase, P^1,P^5-bis(5′-adenosyl) pentaphosphate (AP_5A), tetralithium salts of adenosine 5′-(adenylylimidodiphosphate) (AMPPNP) and adenosine 5′-*O*-(3-thiotriphosphate) (ATPγS), and dithiothreitol were obtained from Boehringer-Mannheim Biochemicals (Indianapolis, IN). Sodium vanadate (Na_3VO_4) was obtained from Fisher Scientific. ATP, ADP, creatine phosphate, hexokinase, and other reagents were obtained from Sigma (St. Louis, MO). The fiber bundles were washed with the following solutions: rigor solution: 190 mM potassium propionate (KPr), 2 mM $MgCl_2$, 1 mM EGTA, and 20 mM 3-(*N*-morpholino)propanesulfonic acid (MOPS) (pH 7.0); ADP solution: rigor solution (180 mM KPr) plus 5 mM MgADP; AMPPNP solution (100 mM ionic strength): 16 mM AMPPNP, 6 mM KPr, 1 mM EGTA, 18 mM $MgCl_2$, 10 mM MOPS (pH 7.0);

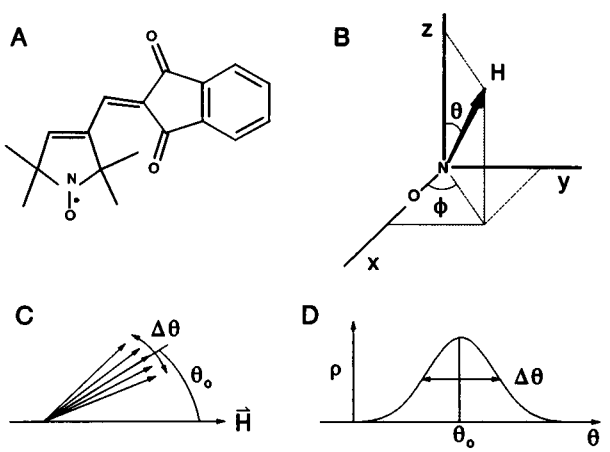

FIGURE 1 (*A*) Chemical structure of InVSL: 2-[oxyl-2,2,5,5,-tetramethylpyrrolin-3-yl)methenyl]indane-1,3-dione. (*B*) Description of the angles θ and ϕ, which define the orientation of the magnetic field *H* with respect to the principal axes of the nitroxide spin label. These angles determine the orientational dependence of the EPR spectrum. (*C* and *D*) Gaussian angular distribution of spin labels, $\rho(\theta_o, \Delta\theta)$, centered at θ_o with a full width at half maximum of $\Delta\theta$.

relaxation solution: 5 mM MgATP, 50 mM creatine phosphate, 750 units/ml creatine kinase in rigor solution (pH 7.0) with 20 mM KPr; contraction solution: relaxation solution plus 1.3 mM $CaCl_2$; ATPγS solution: rigor solution (125 mM KPr plus 25 mM MgATPγS); 200 mM Na_3VO_4 (V_i) stock solution was prepared as described by Barnett and Thomas (1987) and Lewis and Thomas (1986); vanadate solution: 5 mM vanadate in contraction solution (10 mM KPr). The vanadate solution was made before each experiment and was assayed for polymerization by measuring absorbance at 260 nm as described by Lewis and Thomas (1986). Unless otherwise specified, the ionic strength was 200 ± 10 mM in each of these solutions and the pH was adjusted at 25°C. Unless otherwise indicated, preparations and labeling procedures were performed at 4°C; ATPase assays and EPR experiments were carried out at 25 ± 1°C.

Preparations and assays

Subfragment 1 (S1) was prepared by chymotryptic digestion of myosin as described by Roopnarine et al. (1993). S1 was labeled with InVSL as described by Roopnarine et al. (1993). Unlabeled rabbit psoas fiber bundles in a glass capillary (50-μl vol) were decorated with InVSL-S1 in rigor solution as described by Roopnarine and Thomas (1994b). Rabbit psoas fiber bundles were dissected, chemically skinned, and stored as described by Roopnarine and Thomas (1994b). Muscle fiber bundles (~0.5 mm in diameter) were labeled with InVSL at Cys 707 (SH1) and/or Cys 697 (SH2) as described by Roopnarine and Thomas (1994b). SH2-labeled fiber bundles were prepared as described by Roopnarine and Thomas (1994b). Protein concentrations of S1 and myofibrils for ATPase assays and EPR experiments were determined as described by Roopnarine et al. (1993) and Roopnarine and Thomas (1994b). High-salt (K/EDTA- and Ca-) ATPase assays were done as described by Roopnarine et al. (1993). ATPase assays of myofibrils and tension measurements of muscle fibers under physiological conditions were done as described by Roopnarine and Thomas (1995).

We have shown previously, and verified for the InVSL-labeled fibers used in the present study, that 1) essentially all of the spin labels are on the myosin head, 2) most heads have no more than one spin label, 3) about half the spin labels are on SH1, the others on SH2 (Roopnarine et al., 1993; Roopnarine and Thomas, 1994b), and 4) we can obtain corrected EPR spectra corresponding to labels bound specifically to SH1 (Roopnarine and Thomas, 1994b). We have shown that SH1-spin-labeled heads have altered biochemical kinetics, resulting in a higher portion of heads in weak-binding states and correspondingly lower tension; but the labeled heads probably undergo the same structural and chemical transitions as unlabeled heads (Roopnarine and Thomas, 1995; Ostap et al., 1995).

AMPPNP and ATPγS were purified by high-performance liquid chromatography (HPLC) on a preparative Biorad MA7Q (2 cm × 10 cm) (Richmond, CA) anion exchange column as described by Ostap et al. (1995). The purified nucleotides were eluted with a linear gradient of 0–2.0 M triethylamine bicarbonate (pH 7.8). Then the nucleotides were lyophilized, resuspended in distilled water, lyophilized again, and then diluted with distilled water to a final concentration of approximately 100 mM. HPLC analysis showed that the ADP was >99% pure.

EPR spectroscopy

EPR spectra were acquired with a Bruker ESP 300 spectrometer (Bruker Instruments, Billerica, MA) using a TM_{110} cavity that was modified to hold a glass capillary parallel to the magnetic field. The EPR spectra for labeled fibers were acquired with the same instrument settings as described by Roopnarine and Thomas (1994b). EPR spectra with a 100-gauss (G) sweep width were typically acquired, except for some experiments in the presence of AMPPNP, ATPγS, or vanadate, in which the low-field region (25 G) was acquired. Comparison of data analysis from EPR spectra with 100 G and 25 G showed that orientational information was not compromised by acquiring the low-field region. The fiber bundles were perfused with various buffers with a peristaltic pump (except in the ATPγS experiments) as described by Roopnarine and Thomas (1994b). In a typical experiment, the labeled fiber bundles were continuously perfused with 5 mM ADP in rigor solution (pH 7.0) for 1 h to remove noncovalently bound spin label (Roopnarine and Thomas, 1994b), then in 15 mM EDTA in rigor solution for 15 min to remove bound ADP, in rigor solution (pH 7.0), and then in the appropriate nucleotide buffer. The brief incubation in EDTA did not enough to extract troponin C, as determined by sodium dodecyl sulfate polyacrylamide (12%) gel electrophoresis (data not shown) and by the lack of effect on Ca sensitivity of fiber tension and ATPase (Roopnarine and Thomas, 1994b); this is consistent with previous results of others (Moss, 1992).

EPR data analysis

Much of the EPR spectral analysis was carried out with a computer program written by Robert L. H. Bennett. Each EPR spectrum was baseline-corrected by subtracting the spectrum of an unlabeled sample, which was acquired under the same conditions as the labeled sample. The spectrum was normalized to unit spin concentration by dividing the spectrum by the value of its double integral. The spectrum contains contributions from labels bound to both SH1 and SH2; the SH2-bound labels are highly disordered and do not give any orientational information about the myosin head during relaxation or contraction (Roopnarine and Thomas, 1994b). Before analysis involving determination of angular parameters, 60% of the spectrum of SH2-bound InVSL was subtracted, yielding a spectrum of SH1-bound labels, as described by Roopnarine and Thomas (1994b). The angular distribution of spin labels (assuming a Gaussian distribution centered at θ_0 with full width $\Delta\theta$) (Fig. 1, *B–D*) was determined for each component as described by Roopnarine and Thomas (1994b, 1995). Parameter plots showing the dependence of θ_0 and $\Delta\theta$ on the splitting between the zero-crossing of the outer peaks ($2T'$) and ratio of the high-field peak to the center-field peak (Hpp/Cpp) were made from simulated spectra (Roopnarine and Thomas, 1994b) and were used to determine θ_0 and $\Delta\theta$ of the experimental spectrum (Barnett et al., 1986; Fajer et al., 1990a; Roopnarine and Thomas, 1994b).

EPR spectra consisting of different orientational populations were analyzed by fitting them to a linear combination of two endpoint spectra (V_1 and V_2), usually obtained in rigor and relaxation. The mole fractions x_1 and x_2 of V_1 and V_2 were varied, minimizing χ^2 between the composite spectrum ($V_c = x_1V_1 + x_2V_2$) and the experimental spectrum, as described by Roopnarine and Thomas (1995). The fits were acceptable if the difference between the experimental and composite spectra had no significant intensity (<1% compared to the experimental spectrum) (Roopnarine and Thomas, 1995).

RESULTS

ADP

The EPR spectrum of InVSL-labeled fibers in rigor (Fig. 2, *top*) consists of two components, one due to SH1-bound labels and one due to SH2-bound labels (Roopnarine and Thomas, 1994b). The SH1 component, with narrow lines and a wide hyperfine splitting (Fig. 2, *right, top spectrum*), indicates a highly oriented population with the principal axis of the spin label aligned approximately parallel to the fiber axis. The SH2 component has a broad "powder-like" spectrum, implying angular disorder $\Delta\theta$ greater than 90°, and this spectrum is completely insensitive to nucleotides (Roopnarine and Thomas, 1994b, 1995). Therefore, the spectrum of the SH1-bound population in rigor (Fig. 2, *top right*) or any other state was obtained by subtracting 60% of a spectrum of SH2-labeled fibers in rigor (Roopnarine and Thomas, 1994b).

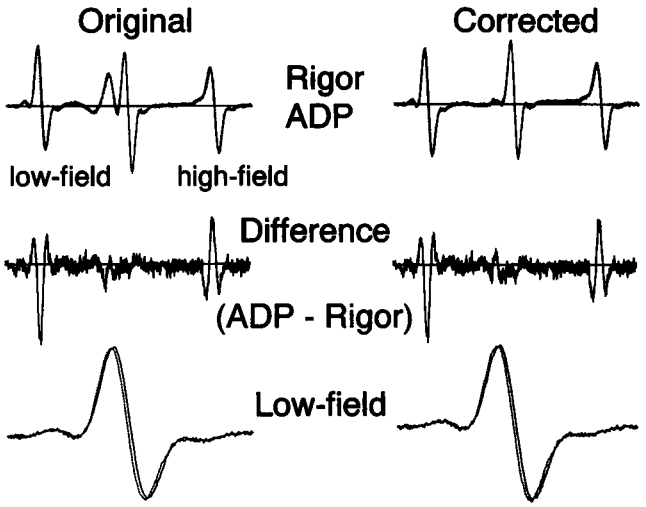

FIGURE 2 EPR spectra of labeled fibers aligned parallel to the magnetic field. (*Top*) Rigor (*solid line*) and ADP (*dotted line*). (*Middle*) ADP spectrum minus rigor spectrum. (*Bottom*) Expanded low-field region of rigor and ADP spectra. Each original spectrum (*top left*) was corrected by subtracting a spectrum of SH2-labeled fibers to give the corrected spectrum (*top right*) of SH1-bound spin labels. The baselines are 100 G wide, except for the expanded low-field region (*bottom*), which is 22.17 G wide.

ADP increased the hyperfine splitting $2T'$, the distance between the zero-crossing points of the low- and high-field lines, from 70.90 ± 0.05 G to 71.45 ± 0.03 G, shifting the low- and high-field lines away from the center-field line (Fig. 2, *dotted line*). This was not due to the presence of contaminating ATP, because 1) HPLC showed the ADP solution to be at least 99% pure, and 2) the addition of an ATP-depleting solution (10 mM glucose, 100 μM AP_5A, and 100 mg/ml hexokinase in ADP solution) had no effect on the spectrum. The change in the hyperfine splitting is shown most clearly by subtracting the rigor spectrum from the ADP spectrum, producing a difference spectrum shaped like a positive derivative at low field and a negative derivative at high field (Fig. 2, *middle*). Analysis of the corrected spectrum (Fig. 2, *right, top spectrum*), corresponding to SH1-bound labels, shows that $2T'$ increased by 0.55 ± 0.02 G (SEM, $n = 8$) on ADP addition. This implies a significant change in θ_0, which is the orientation of the spin label's principal axis relative to the fiber axis (Fig. 1).

Orientational distribution

The effect of ADP on the angular distribution of the SH1-bound spin labels was analyzed using EPR spectral simulations. The spectra in rigor and ADP solutions were each found to be excellent fits to a narrow Gaussian distribution, centered at θ_0 with a full width $\Delta\theta$ (Fig. 1, *C* and *D*). The fit was considered acceptable only if the simulated spectrum had values of the main hyperfine splitting ($2T'$, which is sensitive primarily to θ_0; Barnett et al., 1986) and the ratio of the high-field peak to the center-field peak (Hpp/Cpp, which is sensitive mainly to $\Delta\theta$; Barnett et al., 1986) that were within experimental error of the observed values. The values of θ_0 and $\Delta\theta$ consistent with the data for rigor and rigor + ADP are illustrated in Fig. 3. The acceptable fits for rigor were within the range $\theta_0 = 10$–$12°$ and $\Delta\theta = 13$–$17°$, whereas the values for MgADP were within the range $\theta_0 = 1$–$7°$ and $\Delta\theta = 18$–$23°$. There is no overlap between the regions of parameter space for these two conditions, implying that ADP clearly causes a change in the axial angular distribution, which is most clearly a change in the center of the distribution θ_0 (Fig. 3). The most probable change in θ_0 is 7° (from 11° in rigor to 4° in ADP), but the change in θ_0 could be as low as 3° (from 10° in rigor to 7° in ADP) and as high as 19° (from 12° in rigor to −7° in ADP), because $2T'$ depends only on the values of $\cos^2\theta$.

Effect of ADP on S1-decorated fibers

The EPR spectrum of InVSL-S1 in solution has a "powder" line-shape with a very large hyperfine splitting ($2T_{\parallel}' = 72.35 \pm 0.01$ G), characteristic of strongly immobilized InVSL (Roopnarine et al., 1993). When InVSL-S1 is allowed to flow into a muscle fiber bundle in rigor, it binds to actin in a stereospecific and rigid manner. The resulting spectrum (Fig. 4, *top left*) is similar to that of labeled fibers (Fig. 2, *top left*). The splitting ($2T'$) of the corrected spectrum of SH1-bound spin labels in rigor (Fig. 4, *top right*) was 70.40 ± 0.03 G, which is 0.5 ± 0.1 G less than observed for labeled fibers (Fig. 2, *top right*). Spectral analysis similar to that described above indicate that θ_0 is about 2° greater for extrinsic S1 than for intrinsic heads. The addition of ADP solution to rigor fibers increased $2T'$ to 70.96 ± 0.03 G (Fig. 4), corresponding to an increase (0.56 ± 0.06 G) very similar to that observed for intrinsic heads (0.55 ± 0.2 G; Fig. 2). Thus, although the mean

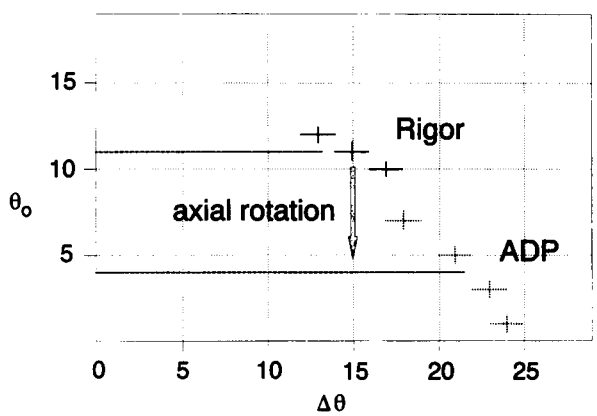

FIGURE 3 Range of possible values for θ_0 and $\Delta\theta$, describing the angular distribution of SH1-bound spin labels in rigor solution and ADP solution, based on the spectra of labeled fibers in Fig. 2. Spectra were simulated, varying θ_0 and $\Delta\theta$ in a 1° grid, and the main hyperfine splitting between the zero crossing points of the outer peaks, $2T'$, and the ratio of the high- to mid-field peaks were measured. The plotted points indicate the values for which both $2T'$ and the peak ratio were within experimental error (SEM) of the experimentally observed values in rigor solution and ADP solution.

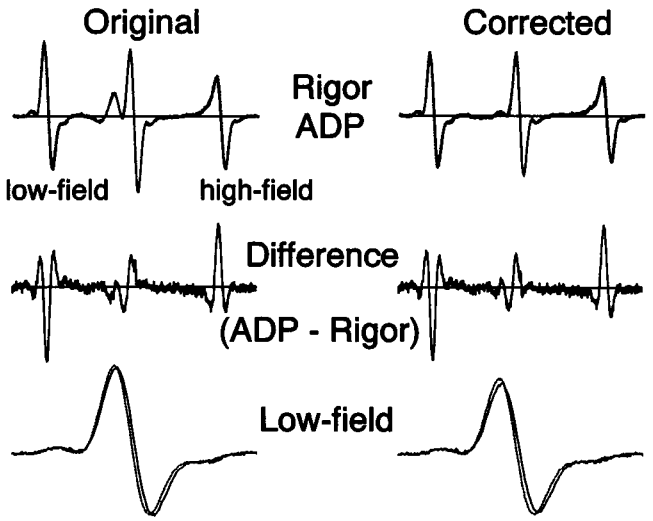

FIGURE 4 EPR spectra of unlabeled fibers decorated with InVSL-S1. (*Top*) Rigor (*solid line*), ADP (*dotted line*). (*Middle*) ADP spectrum minus rigor spectrum. (*Bottom*) Low-field region. Other details as in Fig. 2.

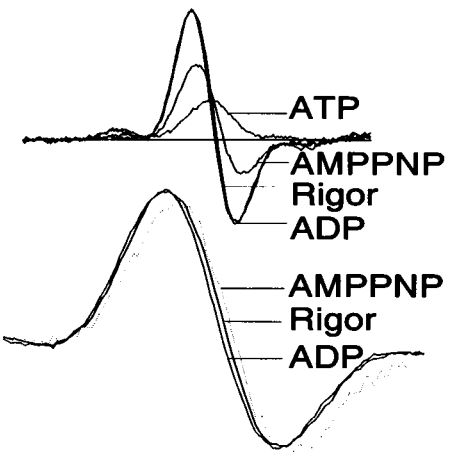

FIGURE 5 AMPPNP effects on low-field region (25.0 G) of spectra of labeled fibers. (*Top*) Overlay of spectra in relaxation (ATP), AMPPNP, rigor, and ADP (*dotted line*). (*Bottom*) Expanded low-field region (12 G) of corrected spectra corresponding to SH1-bound labels in ternary complexes A·M·N (AMPPNP and ADP) and in rigor.

orientation of InVSL at SH1 on an untethered myosin head is slightly different from that of a tethered myosin head, ADP induces a similar small axial rotation in both cases. The intensity of EPR spectrum was unchanged by washing with ADP solution, indicating that ADP did not induce dissociation of actin-attached InVSL-S1. However, the addition of 5 mM MgATP (in rigor solution) to InVSL-S1-decorated fibers eliminated the spectral signal, indicating that ATP dissociated InVSL-S1 and that InVSL-S1 is enzymatically active.

AMPPNP

The addition of AMPPNP solution to labeled fibers in rigor resulted in partial disorder of the SH1-bound spin labels, with clear spectral evidence for at least two orientational populations (Fig. 5). The spectrum was a good fit to a linear combination of spectra obtained in rigor and relaxation, with the best fit giving 0.46 ± 0.02 of the rigor spectrum and 0.54 ± 0.02 of the relaxation spectrum. The difference spectrum between the simulated composite spectrum and the experimental spectrum was negligible (not shown), indicating that there is no significant population of SH1-bound spin labels other than these two populations: a highly ordered population with rigor-like orientation and a highly disordered population like that observed in relaxation. The fractions of the rigor and relaxation components were not changed when the ADP spectrum was used instead of the rigor spectrum in the fitting analysis, but the fit was better (χ^2 smaller) when the rigor spectrum was used, suggesting that θ_o of the ordered component with AMPPNP bound was more similar to rigor than to ADP. Previous studies with MSL (Fajer et al., 1988; Berger and Thomas, 1994) showed that 1) the association constant for AMPPNP binding to spin-labeled actomyosin is 320 M^{-1}, so only 16% of actin-bound heads are without AMPPNP, and 2) the disordered heads in the presence of AMPPNP are all dissociated from actin. To determine the orientation of the ternary complex of A·M·AMPPNP, 16% of the rigor spectrum was subtracted from the ordered component (obtained by subtracting 54% of the relaxation spectrum). The hyperfine splitting corresponding to the ternary complex was 0.5 ± 0.05 G greater than in rigor (Fig. 5, *bottom, AMPPNP spectrum*), indicating θ_o = 13.2 ± 0.6°. The addition of 1.5 mM $CaCl_2$ (resulting in 0.5 mM free Ca) did not affect the spectrum in the presence of AMPPNP.

Pyrophosphate

As in the case of AMPPNP, the addition of 5 mM potassium pyrophosphate (PP_i) to labeled fibers in rigor results in partial disorder, suggesting the conversion of some of the ordered heads to a disordered population (Fig. 6, *third spectrum*). The EPR spectrum was an excellent fit to a linear combination of rigor and relaxation spectra, as shown by the small residual obtained from the difference of the experimental and composite spectra (Fig. 6, *fourth spectrum*). The fraction of disordered SH1-bound spin labels was 0.59 ± 0.02 in rigor solution with 1 mM PP_i. Increasing the PP_i concentration to 5 mM (Fig. 6, *third spectrum*) or 10 mM further increased the SH1-bound disordered fraction to 0.73 ± 0.02. The spectrum of the ordered population of SH1-bound InVSL in the presence of pyrophosphate (not shown) was obtained by subtracting 73% of the relaxation spectrum from the third spectrum in Fig. 6. The splitting $2T'$ was not significantly different from rigor. The addition of 0.3 mM Ca^{2+} to PP_i-bound myosin heads induced a small increase in the ordered population of spin labels (6 ± 0.5%).

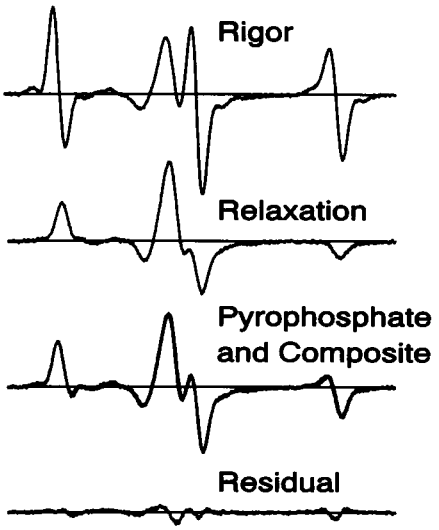

FIGURE 6 Pyrophosphate effects on EPR spectra of labeled fibers. *First spectrum*, rigor; *second spectrum*, relaxation; *third spectrum*, rigor plus 5 mM Mg pyrophosphate, overlaid by the best-fit composite spectrum, made from 73% of the relaxation spectrum plus 27% of the rigor spectrum; *fourth spectrum*, experimental spectrum minus composite spectra.

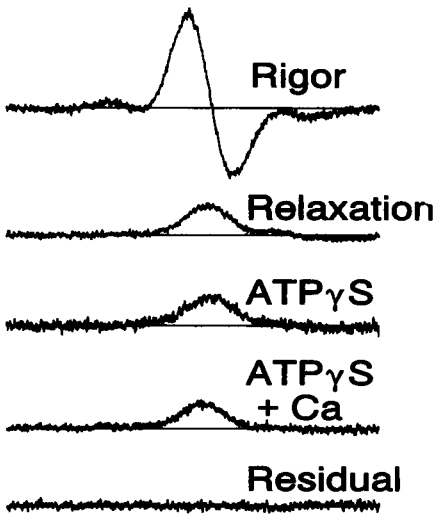

FIGURE 7 ATPγS effects on low-field region (25.0 G) of spectra of labeled fibers. *First spectrum*, rigor (100% ordered); *second spectrum*, relaxation (0% ordered); *third spectrum*, 25 mM ATPγS at 100 mM ionic strength (0% ordered); *fourth spectrum*, 25 mM ATPγS + 0.3 mM Ca at 100 mM ionic strength (6.6% ordered); *fifth spectrum*, fourth spectrum minus the best-fit composite spectrum (93.4% relaxation + 6.6% rigor spectrum). The spectra were normalized to unit concentration before plotting.

ATPγS

The addition of 5 mM MgATPγS to rigor solution (175 mM KPr), in the absence or presence of Ca, induced substantial disorder in the SH1-bound spin labels. EPR spectra were acquired as a function of time to ensure that the accumulation of hydrolysis products did not affect the data and as a function of [ATPγS] (5 to 25 mM, in increments of 5 mM) at different ionic strengths (100 and 200 mM) to achieve nucleotide saturation of myosin heads. In the absence of Ca, at both ionic strengths, the disorder in the EPR spectrum was at maximum at [ATPγS] $\geq$ 25 mM (Fig. 7, *third spectrum*), producing a spectrum identical to that obtained in relaxation at saturating ATP (Fig. 7, *second spectrum*). In the presence of Ca, the EPR spectrum was a good fit to a linear combination of spectra from rigor and relaxation. The addition of 0.5 mM $CaCl_2$ to ATPγS-saturated fibers increased the fraction of ordered spin labels from zero to 3 $\pm$ 1% and 6.6 $\pm$ 1% at 200 and 100 mM ionic strength, respectively (Fig. 7, *fifth spectrum*).

Vanadate

The addition of 5 mM vanadate to fibers in ADP solution had no effect on the highly ordered myosin heads (not shown), but vanadate did have a large disordering effect in the presence of subsaturating ATP (Fig. 8). When the ATP-regenerating system (creatine phosphate and creatine kinase) was omitted from relaxation solution, only 50 $\pm$ 2% of the labeled heads were disordered, with the remaining heads oriented in rigor (Fig. 8, *top left*). When 5 mM vanadate was added to this solution, the oriented (rigor) spectral component was completely eliminated, producing a spectrum (Fig. 8, *top right*) indistinguishable from that observed in relaxation solution (including the ATP-regenerating system) (Fig. 8, *middle left*). This result indicates that the M·ADP·V_i state is orientationally similar to the state in relaxation. The addition of 5 mM vanadate to fibers in relaxation solution had no effect on the EPR spectrum (Fig. 8, *middle right*). In the absence of vanadate, contraction solution produces a spectrum that is a good fit to 79 $\pm$ 2% relaxation (disordered) and 21 $\pm$ 2% rigor (ordered) (Fig. 8, *bottom left*), as we showed previously (Roopnarine and Thomas, 1995). The addition of 5 mM vanadate to contraction solution produced a spectrum that was a good fit to a linear combination of relaxation and rigor, with 6–10%

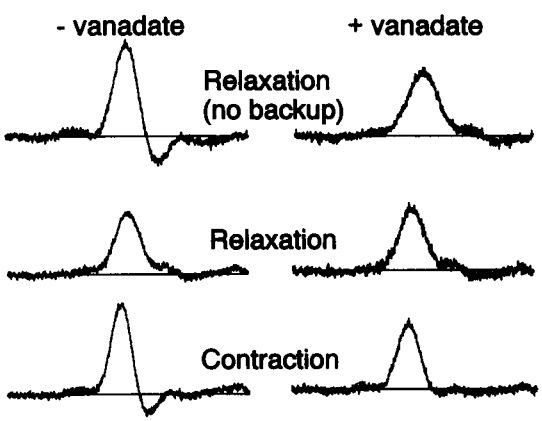

FIGURE 8 Vanadate effects on low-field region (25.0 G) of EPR spectrum of labeled fibers. (*Top*) Relaxation solution minus ATP backup system. (*Middle*) Relaxation solution (includes ATP backup system). (*Bottom*) Contraction solution. (*Right column*) Plus 5 mM vanadate.

ordered (rigor-like) spin labels (Fig. 8, *bottom right*), indicating that M·ADP·V_i myosin heads interact with actin in thin filaments in a Ca^{2+}-dependent manner. After the vanadate-relaxed fibers were washed with rigor solution for 4 min, the normal rigor spectrum was obtained, showing that the formation of the actomyosin bond greatly accelerates the release of vanadate, as observed previously with myosin in solution (Goodno and Taylor, 1982) or in muscle fibers (Dantzig and Goldman, 1985).

DISCUSSION

Many of the experiments in this study are analogous to those done previously using SH1-bound spin labels other than InVSL (Thomas and Cooke, 1980; Fajer et al., 1988, 1990b; Ostap et al., 1995). The primary motivation for this study was to take advantage of InVSL's unique orientation, with its principal axis nearly parallel to the muscle fiber axis in rigor (Roopnarine and Thomas, 1994b). As long as the probe remains rigidly fixed to the protein, any axial rotation of the labeled region of the myosin head by more than 1° should result in the same rotation of the spin label's principal axis, which in virtually every case should be unambiguously detected as a change in the principal hyperfine splitting of the spectrum. This decreased ambiguity is essential in answering a key question posed by the classic rotating cross-bridge model: Is any axial head orientation detectable during force generation that is significantly different from the rigor orientation? We previously used InVSL bound to SH1 to ask this question in the steady state of isometric contraction, concluding that there is a large disordered population of heads during contraction, but there is no significantly populated state with a distinct orientation other than the rigor angle (Roopnarine and Thomas, 1995). In the present study we have used ATP analogs to trap intermediates that might not be highly populated in the steady state, and to ask whether any of these intermediates has a distinct orientation different from rigor. Based on previous work (discussed in the Introduction), the ADP-bound, AMPPNP-bound, and pyrophosphate-bound myosin states have been assigned as part of the force-generating or strong-binding states, whereas the ATPγS- and vanadate-bound myosin states are assigned as part of the preforce or weak-binding states (Scheme 1 and Scheme 2).

Our results are summarized in Table 1 and modeled in Scheme 2, which shows the orientational distributions of myosin heads in different intermediate states of the ATPase cycle, assuming no changes in head shape. In each case, the rigor orientation of the head is shown (solid black) as a reference. The only large orientational changes were increases in the fraction of highly disordered probes. The actin-attached force-producing (strong-binding) states are ordered and rigor-like, and for these states θ_o (center of the distribution of the angle between the fiber axis and the principal axis of the probe for the ternary complex) is indicated in degrees. Since the experiment cannot distinguish between θ_o and $(180°-\theta_o)$, the orientations of the heads were chosen arbitrarily so that ADP release (step 6)

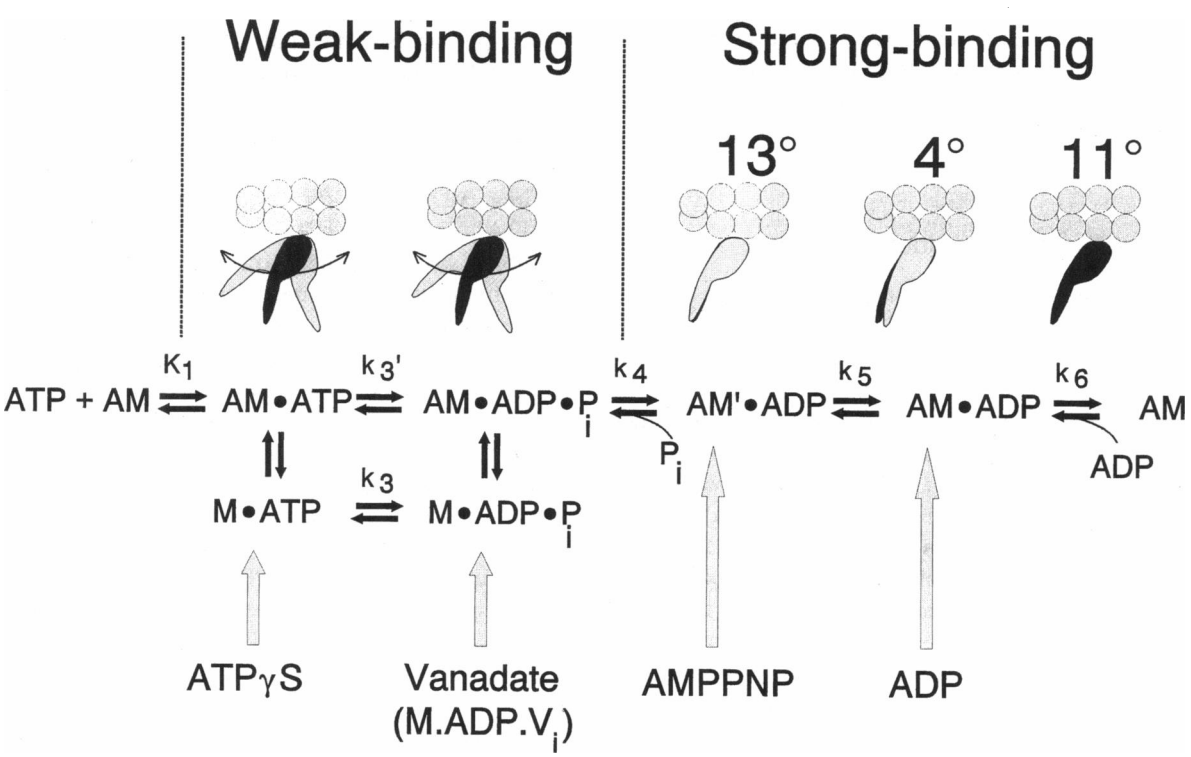

Scheme 2

TABLE 1 Summary of orientational distributions of different nucleotide-bound myosin states

	θ_o (ordered fraction of heads)	% ordered heads
Rigor	11 ± 1°	100%
Relaxation	—	0%
Contraction	8 ± 3°	21 ± 2%
ADP	4 ± 3°	100%
AMPPNP	13.2° ± 0.6°	30 ± 3%
Pyrophosphate	11 ± 1°	27 ± 3%
ATPγS	—	0 ± 0.5%
ATPγS + Ca	—	
Relaxation + vanadate	—	0 ± 0.5%
Contraction + vanadate	7 ± 10°	8 ± 3%

θ_o, the center of the Gaussian distribution of spin label orientations (Fig. 1), and the percentage of ordered heads were obtained by fitting the spectrum of SH1-bound spin labels, after correcting for nucleotide-free (rigor) heads. ATPγS results correspond to 100 mM ionic strength. Results in relaxation and contraction solutions are from Roopnarine and Thomas (1995).

moves the head in the direction of positive force generation. For AMPPNP, only the attached (ordered) population of heads is shown. ADP and AMPPNP both induced oriented actin-attached states differing by a few degrees from the rigor angle. The actin-attached pre-force (weak-binding) states are dynamically disordered by at least 90° on the submillisecond time scale. ATPγS induced a highly disordered state, even in the presence of Ca, when a substantial fraction of heads were attached to actin. Vanadate substantially reduced the fraction of ordered heads during contraction. It is not possible to prove rigorously that these analogs produce complexes that mimic real intermediates in the contractile cycle, but these results provide new support for a model (Scheme 2) in which force generation involves a transition from a disordered state to an ordered (rigor-like) state of myosin head attachment (Thomas et al., 1995), with only very slight differences in orientation of the ordered states.

Strong-binding (force-producing) states

ADP changes the mean axial orientation (θ_o) of the probe's principal axis slightly but significantly, with a most probable change of 7° (Fig. 3, Table 1). Very similar effects of ADP were obtained with fibers decorated with InVSL-labeled S1 (Fig. 4, Table 1), as found previously for other spin labels (Thomas and Cooke, 1980; Fajer et al., 1990b; Ajtai et al., 1992). Therefore, the small axial rotation induced by ADP is independent of the second head and the myosin rod. In light of the mismatch between actin and myosin filament helical symmetries, these results suggest flexibility in a part of myosin that is farther from the actin-binding site than is SH1.

Early studies with a MSL placed an upper bound of 10° on any axial head rotation due to ADP (Thomas et al., 1985; Thomas, 1987). More recently, isotopically substituted MSL derivatives were used to obtain higher orientational resolution in S1-decorated muscle fibers (Fajer et al., 1990b; Ajtai et al., 1992; Fajer, 1994). Those studies reported a detectable effect of ADP on the spin label's orientation, but the change in the most sensitive orientational parameter (the hyperfine splitting) was negligible, implying that the probe's principal axis does not rotate relative to the fiber axis. The principal axis of MSL is nearly perpendicular to the fiber axis, which means that it could be oriented either in the plane of axial head rotation or completely perpendicular to this plane, resulting in ambiguity in deducing head rotation from probe rotation (figure 9 in Roopnarine and Thomas, 1994b). Our present results with InVSL eliminate this ambiguity; InVSL's principal axis lies in the plane of axial head rotation, so the change in the axial orientation of the head cannot be greater than that of the probe's principal axis, indicated by the change in hyperfine splitting. The simplest interpretation of our data is that ADP induces an axial rotation of the myosin head, with a most probable rotation of 7°. However, two other sources of probe rotation are also plausible: 1) The observed rotation could be due to an internal structural change within the catalytic domain of the head, as detected with other SH1-bound probes (Barnett and Thomas, 1987; Tanner et al., 1992; Raucher et al., 1994; Ostap et al., 1995). This is not likely in the case of InVSL, because SH1-bound InVSL has no nanosecond and microsecond rotational mobility relative to S1, in the presence or absence of nucleotides (Roopnarine et al., 1993). 2) A torsional rotation, about the long axis of the myosin head, could also affect the spectral hyperfine splitting. Because InVSL's principal axis is at roughly a 45° angle to the head, and the head axis is at roughly a 45° angle to the fiber axis, a torsional rotation of the head would result in an axial rotation of the probe, as suggested by previous studies with other spin labels (Ajtai et al., 1992; Fajer, 1994; Raucher et al., 1994). Thus the observed 7° axial rotation of InVSL's principal axis is a strict *upper bound* for the axial rotation of the myosin head due to ADP.

The AM·ADP state we are studying here, produced by adding ADP to rigor, is probably not the same as AM′·ADP, the proposed force-generating state that can combine with phosphate to reverse force production and ATP hydrolysis (Schemes 1 and 2) (Sleep and Hutton, 1980; Dantzig et al., 1991). The reaction of AM·ADP with phosphate to produce ATP is minimal (Sleep and Hutton, 1980; Dantzig and Goldman, 1985), and ADP decreases rigor tension by only 15% (Tanner et al., 1992). The very small ADP-induced rotation we have detected probably corresponds to the reversal of a step (AM·D → AM) that occurs very late in the power stroke, after most force has already been generated.

In the presence of AMPPNP, about half of the SH1-bound spin labels (heads) were highly disordered, whereas the rest remained ordered, almost as in rigor (Fig. 5, Table 1). Thus, although AMPPNP is not hydrolyzed by myosin, it disrupts the ordered assembly of actin-attached myosin heads in rigor. The most likely interpretation is that most of the labeled heads are in equilibrium between two orientational states, an actin-detached M·AMPPNP state with dis-

order similar to that of relaxation and an actin-attached AM·AMPPNP state with order similar to that of rigor. This is consistent with the millisecond detachment/attachment equilibrium deduced from stiffness measurements in the presence of AMPPNP (Schoenberg and Eisenberg, 1985), but the millisecond time scale is slow (effectively static) compared with 1) the microsecond rotational motion of detached heads (Fajer et al., 1988) and 2) the nanosecond exchange that would be required to average the two EPR spectral components. Thus, EPR is sensitive to the equilibrium constant but not to the rate constants for attachment and detachment.

Our observation of a stereospecific, rigor-like orientation of probes in the ternary complex AM·AMPPNP is consistent with previous EPR studies with MSL in fibers (Fajer et al., 1988). The present study does more than confirm this result. Because of InVSL's unique orientation, there is sufficient sensitivity to show that the axial orientation in the ternary complex AM·AMPPNP (13.2 ± 0.6°) is significantly different from that in rigor (11 ± 1°), and the change is in the direction opposite that induced by ADP (4 ± 3°). Our conclusion, that AMPPNP dissociates some heads from actin and induces a slight structural change in the remaining cross-bridges, is consistent with electron microscopic investigations of AMPPNP effects on insect flight muscle (Taylor et al., 1993).

Pyrophosphate has an effect similar to that of AMPPNP, detaching and disordering a portion of the heads, with the ternary complex remaining rigor-like (Fig. 6, Table 1), as shown previously using MSL (Cooke and Pate, 1988). However, in contrast to AMPPNP, pyrophosphate did not cause a significant change in the orientation of the ordered population, suggesting that the β and γ phosphates are sufficient to weaken the actomyosin bond, but not to reorient the heads that remain bound—adenine is also required for the latter.

Weak-binding (non-force-producing) states

In the presence of 25 mM ATPγS, heads are disordered as in relaxation (Fig. 7), but the addition of Ca induces a small fraction (6.6%) of rigor-like ordered heads in 100 mM ionic strength. This is small compared to the 21 ± 1% ordered heads observed in contraction (200 mM ionic strength) (Roopnarine and Thomas, 1995). The hydrolysis step for ATPγS on myosin is very slow, presumably keeping most of the heads in a state that mimics the prehydrolysis (A)M·ATP state (Schemes 1 and 2). ATPγS probably binds to myosin heads more weakly in the presence of Ca (Kraft et al., 1992; Resetar and Chalovich, 1995), so it is possible that the small ordered (rigor-like) fraction (6.6 ± 1% at 100 mM ionic strength) is due to nucleotide-free (rigor) heads. Berger and Thomas (1994) used the proteolytic susceptibility property of nucleotide-bound myosin heads to determine the fraction of actin-bound heads in spin-labeled myofibrils in the presence of ATPγS. Based on that study, the fraction of actin-bound heads under our experimental conditions at 100 mM ionic strength is 23 ± 6%. This is much greater than the 6.6 ± 1% ordered fraction detected in the present study, so most of the actin-bound heads in the ternary complex AM·ATPγS are disordered as in relaxation. Our finding that ATPγS induces disorder in actin-attached myosin heads is consistent with previous studies with MSL showing that the ternary complex of AM·ATPγS has microsecond dynamic disorder similar to relaxation (Berger and Thomas, 1994; Fajer et al., 1995). This result suggests that myosin heads are highly disordered early in weak-binding states that occur early in the ATPase cycle, as suggested by transient EPR studies of contracting fibers (Roopnarine and Thomas, 1994a).

Vanadate did not affect the orientational distribution in rigor or in the presence of ADP, but did induce disorder in activated fibers, both in the presence of subsaturating ATP (Fig. 8, *top*) or in contraction solution (Fig. 8, *bottom*). This is consistent with previous mechanical (Dantzig and Goldman, 1985) and EPR (Ostap et al., 1995) studies, which showed that the vanadate-bound state is populated only when the cross-bridges are cycling through the ATPase kinetic cycle; vanadate binds to the AM′·ADP state and reverses step 4 (Scheme 2), reducing the force. We conclude that vanadate binds to myosin heads that are in the ordered (rigor-like) AM′·ADP state (strong-binding, force-producing) and forms the disordered (A)M·ADP·V_i state, which mimics the (A)M·ADP·P_i state (weak-binding, non-force-producing) (Scheme 2).

Our results indicate that 1) the adenine moiety is required to change the axial orientation of the head significantly, because neither pyrophosphate nor vanadate alone is sufficient to cause a significant change in the angle of the ordered spectral component, and that 2) both the β and γ phosphates are required to weaken and disorder the actomyosin bond substantially, because neither ADP nor vanadate alone depletes the ordered component in the EPR spectrum (Table 1).

Molecular models for force generation

The present results on equilibrium states trapped with nucleotide analogs, coupled with our previous results in rigor, relaxation, and contraction, support a model for contraction involving a transition from a dynamically disordered, weakly bound preforce state to an ordered (rigor-like), strongly bound force-generating state, accompanied by slight changes in the axial orientation of the catalytic domain (Thomas et al., 1995; Ostap et al., 1995; Roopnarine and Thomas, 1995). Scheme 2 illustrates this model, in the context of the results of the present study. Scheme 2 is consistent with the x-ray crystal structural analyses of S1 (Rayment et al., 1993a,b) and S1 fragments containing nucleotide analogs (Fisher et al., 1995a,b; Smith and Rayment, 1995), which have produced suggestions for how nucleotide binding, hydrolysis, and release induce a series

of subtle structural changes within the catalytic domain, leading to changes in actomyosin affinity and to force generation. That model suggests, consistently with Scheme 2, that the initial attachment of S1 to actin in weak-binding states is not stereospecific (Rayment et al., 1993a,b). The slight effect we observe with ADP (reversal of step 6) is consistent with the small structural perturbation that the adenine moiety induces within the catalytic domain (Fisher et al., 1995a,b; Smith and Rayment, 1995). The larger effects we observe with ATP·vanadate and with ATPγS (reversal of steps 4 and 3) are consistent with the more substantial changes within the catalytic domain and the actomyosin interface that appear to require the presence of all three phosphates (Fisher et al., 1995a,b; Smith and Rayment, 1995). The x-ray analysis also suggests that significant structural changes within the catalytic domain are induced by ATP hydrolysis (step 3 in Scheme 2). Because InVSL reports only global orientation of the catalytic domain, this effect is not resolved in the present study, but a complementary EPR study with IASL (sensitive to local structural changes near SH1) confirmed that a structural change occurs within the catalytic domain in step 3 (Ostap et al., 1993, 1995).

In summary, the EPR and x-ray crystallography results are consistent with Scheme 2, in which force is generated by a series of subtle structural changes within the catalytic domain, coupled to a disorder-to-order transition. However, this would be sufficient to produce force only if the mean orientation in the disordered (weak-binding) heads were substantially different from that of the ordered (strong-binding) heads. We have shown (Roopnarine and Thomas, 1995) that the mean orientation of the disordered heads in contraction is probably rigor-like, as depicted in Scheme 2. Therefore, it is necessary to consider a model in which subtle conformational changes within the catalytic domain, where SH1 resides, are coupled to a more substantial change in the shape of the head, resulting in a rotation of the light-chain-binding domain, between the catalytic domain and myosin rod (Huxley and Kress, 1985; Cooke, 1986; Rayment et al., 1993b; Smith and Rayment, 1995). Fig. 9 depicts a model for the force-generating step that combines the disorder-to-order transition with the internal bending of the head. This model is supported by EPR and phosphorescence studies of labeled regulatory light chains, indicating rotational motion of the light-chain-binding domain relative to the catalytic domain in contraction (Hambly et al., 1992; Thomas et al., 1995; Roopnarine et al., 1995), fluorescence polarization of labeled regulatory light chains, showing tilting motions that correlate with force changes during mechanical transients (Irving et al., 1995), and electron microscopic analysis of S1-decorated actin filaments, showing that ADP appears to induce a substantial tilt of the light-chain-binding domain relative to the catalytic domain (Whittaker et al., 1996; Jontes et al., 1996). Spectroscopic studies of labeled light chains are required to test this model further.

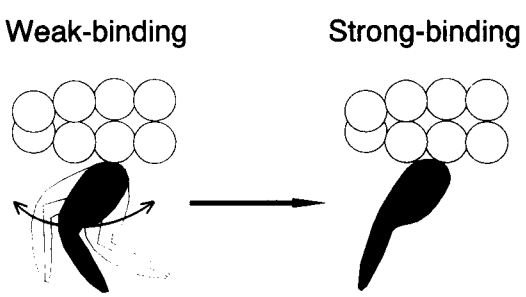

FIGURE 9 A model for the force-generating step that combines the disorder-to-order transition with internal bending of the head. In weak-binding (pre-force) states, heads are dynamically disordered and bent, but the mean orientation of the catalytic domain is the same as in rigor. In strong-binding (force-producing) states, heads are rigidly oriented and straight.

We thank Robert L. H. Bennett for development of EPR data analysis software and spectrometer maintenance, Edmund C. Howard for improvements in EPR fitting and simulation programs, and Franz L. Nisswandt and Nicoleta Cornea for development and maintenance of other computational hardware and software. All of the above are affiliated with the University of Minnesota Medical School (Minneapolis, MN). We are especially indebted to Dr. Kálmán Hideg, University of Hungary at Pécs, for generously providing us with the spin label InVSL.

This work was supported by grants to D. Thomas from the National Institutes of Health (AR32961), the Muscular Dystrophy Association, and the Minnesota Supercomputer Institute.

REFERENCES

Ajtai, K., A. Ringler, and T. P. Burghardt. 1992. Probing cross-bridge angular transitions using multiple extrinsic reporter groups. *Biochemistry.* 31:207–217.

Bagshaw, C. R., J. F. Eccleston, D. R. Trentham, D. W. Yates, and R. S. Goody. 1972. Transient kinetic studies of the Mg^{++}-dependent ATPase of myosin and its proteolytic subfragments. *Cold Spring Harb. Symp. Quant. Biol.* 37:127–135.

Barnett, V. A., P. G. Fajer, C. F. Polnaszek, and D. D. Thomas. 1986. High-resolution detection of muscle crossbridge orientation by electron paramagnetic resonance. *Biophys. J.* 49:144–146.

Barnett, V. A., and D. D. Thomas. 1987. Resolution of conformational states of spin-labeled myosin during steady-state ATP hydrolysis. *Biochemistry.* 26:314–323.

Barrington-Leigh, J., K. C. Holmes, H. G. Mannherz, G. Rosenbaum, F. Eckstein, and R. S. Goody. 1972. Effects of ATP analogs on the low-angle X-ray diffraction pattern of insect flight muscle. *Cold Spring Harb. Symp. Quant. Biol.* 37:443–448.

Berger, C. L., and D. D. Thomas. 1994. Rotational dynamics of actin-bound intermediates of the myosin ATPase cycle in myofibrils. *Biophys. J.* 67:250–261.

Cooke, R. 1986. The mechanism for muscle contraction. *CRC Crit. Rev. Biochem.* 21:53–118.

Cooke, R., M. S. Crowder, and D. D. Thomas. 1982. Orientation of spin labels attached to cross-bridges in contracting muscle fibers. *Nature.* 300:776–778.

Cooke, R., and E. Pate. 1988. Energetics of the actomyosin bond in the filament array of muscle fibers. *Biophys. J.* 53:561–573.

Dantzig, J. A., and Y. E. Goldman. 1985. Suppression of muscle contraction by vanadate. *J. Gen. Physiol.* 86:305–327.

Dantzig, J. A., Y. E. Goldman, N. C. Millar, and E. Homsher. 1992. Reversal of the cross-bridge force-generating transition by photogeneration of phosphate in rabbit psoas muscle fibres. *J. Gen. Physiol.* 451:247–278.

Dantzig, J. A., M. G. Hibberd, D. R. Trentham, and Y. E. Goldman. 1991. Cross-bridge kinetics in the presence of MgADP investigated by photolysis of caged ATP in rabbit psoas muscle fibers. *J. Physiol.* 432: 639–680.

Dantzig, J. A., J. W. Walker, D. R. Trentham, and Y. E. Goldman. 1988. Relaxation of muscle fibers with adenosine 5′-[γ-thio]triphosphate (ATP[γS]) and by laser photolysis of caged ATP[γS]: evidence for Ca^{2+}-dependent affinity of rapidly detaching zero-force cross-bridges. *Proc. Natl. Acad. Sci. USA.* 85:6716–6720.

Fajer, P. G. 1994. Method for the determination of myosin head orientation from EPR spectra. *Biophys. J.* 66:2039–2050.

Fajer, P. G., R. L. H. Bennett, C. F. Polnaszek, E. A. Fajer, and D. D. Thomas. 1990a. General method for multiparameter fitting of high-resolution EPR spectra using a simplex algorithm. *J. Magn. Reson.* 88:111–125.

Fajer, P. G., E. A. Fajer, N. J. Brunsvold, and D. D. Thomas. 1988. Effects of AMPPNP on the orientation and rotational dynamics of spin-labeled muscle cross-bridges. *Biophys. J.* 53:513–524.

Fajer, P. G., E. A. Fajer, J. J. Matta, and D. D. Thomas. 1990b. Effect of ADP on the orientation of spin-labeled myosin heads in muscle fibers: a high resolution study with deuterated spin labels. *Biochemistry.* 29: 5865–5871.

Fajer, P. G., E. A. Fajer, M. Schoenberg, and D. D. Thomas. 1991. Orientational disorder and motion of weakly attached cross-bridges. *Biophys. J.* 60:642–649.

Fajer, P. G., E. A. Fajer, and D. D. Thomas. 1990c. Myosin heads have a broad orientational distribution during isometric muscle contraction. Time-resolved EPR studies using caged ATP. *Proc. Natl. Acad. Sci. USA.* 87:5538–5542.

Fajer, E. A., E. M. Ostap, D. D. Thomas, N. Naber, and P. Fajer. 1995. Orientation and dynamics of myosin heads in ATPγS and Ca^{2+}. *Biophys. J.* 68:322s.

Fisher, A. J., C. A. Smith, J. Thoden, R. Smith, K. Sutoh, H. M. Holden, and I. Rayment. 1995a. Structural studies of myosin: nucleotide complexes: a revised model for the molecular basis of muscle contraction. *Biophys. J.* 68:19s–28s.

Fisher, A. J., C. A. Smith, J. Thoden, R. Smith, K. Sutoh, H. M. Holden, and I. Rayment. 1995b. X-ray structures of the myosin motor domain of *Dictyostelium discoidium* complexed with MgADP·BeF_x and MgADP·ALF_4^-. *Biochemistry.* 34:8960–8972.

Goody, R. S., K. C. Holmes, M. G. Mannherz, J. Barrington-Leigh, and G. Rosenbaum. 1975. Crossbridge conformation as revealed by X-ray diffraction studies on insect flight muscles with ATP analogues. *Biophys. J.* 15:687–705.

Goodno, C. C. 1979. Inhibition of myosin ATPase by vanadate ion. *Proc. Natl. Acad. Sci. USA.* 76:2620–2624.

Goodno, C. C., and E. W. Taylor. 1982. Inhibition of actomyosin ATPase by vanadate. *Proc. Natl. Acad. Sci. USA.* 79:21–25.

Greene, L. E., and E. Eisenberg. 1978. Formation of a ternary complex: actin, 5′-adenylyl imidodiphosphate, and the subfragments of myosin. *Proc. Natl. Acad. Sci. USA.* 75:54–58.

Hambly, B., K. Franks, R. Cooke. 1992. Paramagnetic probes attached to a light chain on the myosin head are highly disordered in active muscle fibers. *Biophys. J.* 63:1306–1313.

Hankovszky, H. O., K. Hideg, and G. Jerkovich. 1989. Synthesis of 3-substituted 2,5-dihydro-2,2,5,5-tetramethyl-1H-pyrrol-1-yloxyl radicals, useful for spin-labeling of biomolecules. *Synthesis.* 7:526–529.

Huxley, A. F., and R. Simmons. 1971. Proposed mechanism of force generation in striated muscle. *Nature.* 233:533–538.

Huxley, H. E. 1969. The mechanism of muscular contraction. *Science.* 114:1356–1366.

Huxley, H. E., and M. Kress. 1985. Crossbridge behavior during muscle contraction. *J. Muscle Res. Cell Motil.* 6:153–161.

Irving, M., T. St. C. Allen, C. Sabido-David, J. S. Craik, B. Brandemeier, J. Kendrick-Jones, J. E. T. Corrie, D. R. Trentham, and Y. E. Goldman. 1995. Tilting of the light-chain region of myosin during step length changes and active force generation in skeletal muscle. *Nature.* 375: 688–691.

Jontes, J. D., E. M. Wilson-Kubalek, and R. A. Milligan. 1996. A 32° tail swing in brush border myosin I on ADP release. *Nature.* 378:751–753.

Kraft, T., L. C. Yu, H. J. Kuhn, and B. Brenner. 1992. Effect of Ca^{2+} on weak crossbridge interaction with actin in the presence of adenosine 5′-[γ-thio]triphosphate. *Proc. Natl. Acad. Sci. USA.* 89:11362–11366.

Kuhn, H. J. 1978. Tension transients in fibrillar muscle fibres as affected by stretch-dependent binding of AMPPNP: a teinochemical effect? *Biophys. Struct. Mech.* 4:209–222.

Lewis, S. M., and D. D. Thomas. 1986. Effects of vanadate on the rotational dynamics of spin-labeled calcium adenosinetriphosphatase in sarcoplasmic reticulum membranes. *Biochemistry.* 25:4615–4621.

Marston, S. B., C. D. Rodger, and R. T. Tregear. 1976. Changes in muscle cross-bridges when AMPPNP binds to myosin. *J. Mol. Biol.* 104:263–276.

Morales, M. F., and J. Botts. 1979. On the molecular basis for chemomechanical energy transduction in muscle. *Proc. Natl. Acad. Sci. USA.* 76:3857–3859.

Moss, R. 1992. Ca^{2+} regulation of mechanical properties of striated muscle: mechanistic studies using extraction and replacement of regulatory proteins. *Circ. Res.* 70:865–884.

Ostap, E. M., V. A. Barnett, and D. D. Thomas. 1995. Resolution of three structural states of spin-labeled myosin in contracting muscle. *Biophys. J.* 69:177–188.

Ostap, E. M., H. D. White, and D. D. Thomas. 1993. Transient detection of spin-labeled myosin subfragment 1 conformational states during ATP hydrolysis. *Biochemistry.* 32:6712–6720.

Raucher, D. M., C. P. Sar, K. Hideg, and P. G. Fajer. 1994. Myosin catalytic domain flexibility in MgADP. *Biochemistry.* 33:14317–14323.

Rayment, I., H. M. Holden, M. Whittaker, C. B. Yohn, M. Lorenz, K. C. Holmes, and R. A. Milligan. 1993a. Structure of the actin-myosin complex and its implications for muscle contraction. *Science.* 261: 58–65.

Rayment, I., W. R. Rypniewski, K. Schmidt-Bäse, R. Smith, D. R. Tomchick, M. M. Benning, D. A. Winklemann, G. Wesenberg, and H. M. Holden. 1993b. Three-dimensional structure of myosin subfragment-1: a molecular motor. *Science.* 261:50–58.

Reedy, M. K., K. C. Holmes, and R. T. Tregear. 1965. Induced changes in orientation of the cross-bridge glycerinated insect flight muscle. *Nature.* 297:1276–1280.

Reedy, M. C., M. K. Reedy, and R. S. Goody. 1983. Coordinated electron microscopy and X-ray studies of glycerinated insect flight muscle. II. Electron microscopy and image reconstruction of muscle fibers fixed in rigor, in ATP, and in AMPPNP. *J. Muscle Res. Cell Motil.* 4:55–81.

Resetar, A. M., and J. M. Chalovich. 1995. Adenosine 5′-(gamma-thiotriphosphate): an ATP analog that should be used with caution in muscle contraction studies. *Biochemistry.* 34:16039–16045.

Roopnarine, O., K. Hideg, and D. D. Thomas. 1993. Saturation transfer EPR spectroscopy with an indane dione spin label: calibration with hemoglobin and application to myosin rotational dynamics. *Biophys. J.* 64:1986–1907.

Roopnarine, O., A. G. Szent-Györgyi, and D. D. Thomas. 1995. Saturation transfer electron paramagnetic resonance of spin-labeled myosin regulatory light chains in contracting muscle fibers. *Biophys. J* 68:337s.

Roopnarine, O., and D. D. Thomas. 1994a. Myosin heads are disordered early in the ATPase cycle in spin-labeled rabbit muscle fiber bundles. *Biophys. J.* 66:A234.

Roopnarine, O., and D. D. Thomas. 1994b. A spin label that binds to myosin heads in muscle fibers with its principal axis parallel to the fiber axis. *Biophys. J.* 67:1634–1645.

Roopnarine, O., and D. D. Thomas. 1995. Orientational dynamics of indane dione spin-labeled myosin head in relaxed and contracting skeletal muscle fibers. *Biophys. J.* 68:1461–1471.

Schoenberg, M., and E. Eisenberg. 1985. Muscle cross-bridge kinetics in rigor and in the presence of ATP analogues. *Biophys. J.* 48:863–871.

Sleep, J. A., and R. I. Hutton. 1980. Exchange between inorganic phosphate and adenosine 5′-triphosphate in the medium by actomyosin subfragment 1. *Biochemistry.* 19:1276–1283.

Smith, C. A., and I. Rayment. 1995. X-ray structure of the magnesium(II)-pyrophosphate complex of the truncated head of *Dictyostelium discoidium* myosin to 2.7 Å resolution. *Biochemistry.* 34:8973–8981.

Tanner, J. W., D. D. Thomas, and Y. E. Goldman. 1992. Transients in orientation of a fluorescent cross-bridge probe following photolysis

of caged nucleotides in skeletal muscle fibres. *J. Mol. Biol.* 223: 185–203.

Taylor, K. A., M. C. Reedy, M. K. Reedy, and R. A. Crowther. 1993. Crossbridges in the complete unit cell of rigor insect flight muscle imaged by three-dimensional reconstruction from oblique sections. *J. Mol. Biol.* 233:86–108.

Thomas, D. D. 1987. Spectroscopic probes of muscle cross-bridge rotation. *Annu. Rev. Physiol.* 49:891–909.

Thomas, D. D., and R. Cooke. 1980. Orientation of spin-labeled myosin heads in glycerinated muscle fibers. *Biophys. J.* 32:891–906.

Thomas, D. D., S. Ramachandran, O. Roopnarine, D. W. Hayden, and E. M. Ostap. 1995. The mechanism of force generation in myosin: a disorder-to-order transition, coupled to internal structural changes. *Biophys. J.* 68:135s–141s.

Thomas, D. D., E. C. Svensson, and C. F. Polnaszek. 1985. ADP does not induce rigid axial rotation of myosin heads in rigor muscle fibers. *Biophys. J.* 47:380a.

Whittaker, M., E. M. Wilson-Kubalek, J. E. Smith, L. Faust, R. A. Milligan, and H. L. Sweeney. 1996. A 35-Å movement of smooth muscle on ADP release. *Nature.* 378:748–751.

Xu, S., B. Brenner, and L. C. Yu. 1993. State-dependent radial elasticity of attached cross-bridges in single skinned fibres of rabbit psoas muscle. *J. Physiol. (Lond.).* 465:749–765.